Supporting Information

Exploring the insertion mechanism of pseudocapacitive perovskite oxide La-Ni-Co-O anode materials and the application to Li-ion capacitor and Li-based dual ion batteries

Yi Li[1], Yuxi Huang[1], Rui Ding, Caini Tan, Jian Guo, Yiqing Lu, Zhiqiang Chen, Yibo Zhang and Runzhi Xu*

Key Laboratory of Environmentally Friendly Chemistry and Applications of Ministry of Education, College of Chemistry, Xiangtan University, Xiangtan, Hunan 411105, P.R. China.

[1]The authors contribute equally to the work.

Corresponding author

[*]E-mails: drm8122@xtu.edu.cn; drm8122@163.com

Table of Contents

Fig S10. Performance of LNCO(1:1)/LO electrode with A electrolytes: CV plots for the first three cycles at 0.3 mV s^{-1} (a), GCD curves at 0.1 A g^{-1} for the first five cycles (b), GCD curves at 0.1-3.2 A g^{-1} (c), specific capacity and coulombic efficiency at 0.1-3.2 A g^{-1} (d), and cycling behavior at 2 A g^{-1} (e).

Fig S11. Performance of LNCO(1:3)/LO electrode with A electrolytes: CV plots for the first three cycles at 0.3 mV s^{-1} (a), GCD curves at 0.1 A g^{-1} for the first five cycles (b), GCD curves at 0.1-3.2 A g^{-1} (c), specific capacity and coulombic efficiency at 0.1-3.2 A g^{-1} (d), and cycling behavior at 2 A g^{-1} (e).

Fig S12. Performance of LNCO(0:1)/LO electrode with A electrolytes: CV plots for the first three cycles at 0.3 mV s^{-1} (a), GCD curves at 0.1 A g^{-1} for the first five cycles (b), GCD curves at 0.1-3.2 A g^{-1} (c), specific capacity and coulombic efficiency at 0.1-3.2 A g^{-1} (d), and cycling behavior at 2 A g^{-1} (e).

Fig S13. Performance of LNCO(1:3)/LO//AC LICs with A electrolytes: CV windows at 10 mV s^{-1} (a), CV plots at 10~160 mV s^{-1} in 4.0 V (b), 4.3 V (c), 4.5 V (d).

Fig S14. Performance of LNCO(1:3)/LO//KS6 DIBs with A electrolytes: CV windows at 10 mV s^{-1} (a), CV plots at 10~160 mV s^{-1} in 5.0 V (b), 5.2 V (c).

Fig S15. GCD curves of LNCO(1:3)/LO//KS6 DIBs and LNCO(1:3)/LO//AC LICs with A electrolytes: GCD curves at 0.5-8.0 A g^{-1} in 5.0 V (a), 5.2 V (b) of LNCO(1:3)/LO//KS6 Li-DIBs; GCD curves at 0.5-16.0 A g^{-1} in 4.0 V (c), 4.3 V (d), 4.5V (e) of LNCO(1:3)/LO//AC LICs.

Supplemental Tables

Table S1. Chemicals, agents and materials used in the study.

Table S2. Specific capacity and cycling retention of the LNCO/LO(Ni:Co=1:0~0:1) electrodes.

Table S3. Specific capacity cycling retention of AC and KS6 electrodes.

Table S4. Performance summary of the LICs and Li-DIBs in the study under room temperature (25 ^{o}C), m^{+}/m^{-}=1:1.

Table S5. A comparison for the performance of the LNCO(1:3)/LO//AC LICs in the study with some reported LICs.

Table S6. A comparison for the performance of the LNCO(1:3)/LO//KS6 Li-DIBs in the study with some reported Li-DIBs.

References.

Experimental Procedures

Synthesis of LNCO materials

The chemicals in the experiment were of analytical level (A.R.) and directedly used without further treatment (**Table S1**). The LNCO samples were synthesized via precipitation route. Take the procedure of LNCO(1:3) for an example. Firstly, 1.0 mmol $La(NO_3)_3{\cdot}xH_2O$, 0.25 mmol $Ni(NO_3)_2{\cdot}6H_2O$ and 0.75 mmol $Co(NO_3)_2{\cdot}6H_2O$ were dissolved in 50 mL deionized water, and the mixture was stirred magnetically until fully dispersed. Secondly, a mixture of 2 mol L^{-1} NaOH and 1 mol L^{-1} Na_2CO_3 was added to the solution and the pH was adjusted to 10. After standing age for 4 h, it was washed with deionized water for several times and collected by vacuum filtration. The precursor products were dried overnight at 100 ℃ and calcined in muff furnace at 700 ℃ for 6 h to obtain the products. The other four LNCO samples (1:0, 3:1, 1:1 and 0:1) were also synthesized as the procedure described above except by using different stoichiometric molar ratios of Ni:Co at the beginning. (The above-mentioned chemicals, agents and materials are listed in the **Table S1**.)

Characterizations

The phases and crystallinity properties were determined by X-ray diffraction (XRD). The surface structures were checked by X-ray photoelectron spectra (XPS). The morphology and size of particles were analyzed by scanning electron microscopy (SEM) and transmission electron microscopy (TEM). The crystalline microstructures were resolved by the high-resolution TEM (HRTEM) and selected area electron diffraction (SAED). The element composition and distribution were measured by the X-ray energy dispersive spectra (EDS), inductively coupled plasma-optical emission spectrometer (ICP-OES) and mapping. The specific surface area, pore volume and size distribution were examined by nitrogen isothermal sorptions with Brunauer-Emmett-Teller (BET) and Barrett-Joyner-Halenda (BJH) methods.

Electrochemical measurements

The electrodes were prepared by the following two steps: firstly, A well-dispersed mixture of 70 wt% active materials (as-synthesized LNCO(1:0~0:1) or commercial AC or KS6 , 20 wt% acetylene black (AB) conductive agent and 10 wt% polyvinylidene fluoride binder (PVDF, which was dissolved in into the N-methyl-2-pyrrolidone (NMP)) were casted onto the current collectors (Cu foil and carbon-coated Al foil were used for the collectors of anode and cathode respectively), and followed by drying in a vacuum oven at 110 °C for 12 h; secondly, the electrodes were pounched into disks with diameter of 12 mm, and the mass loading of active materials was about 1.2~4.5 mg cm^{-2}. The electrochemical performances were examined via CHI 660E electrochemical working stations and Neware-CT-4008 testers. Tests for electrodes (LNCO/LO, AC, KS6,) were conducted in halfcells by using the type 2032 coin cells. Tests for LICs (LNCO(1:3)/LO//AC) and Li-DIBs (LNCO(1:3)/LO//KS6) were conducted via full-cells with type 2032 coin cells, with certain mass ratios of anode and cathode

active materials (**Tables S2-4**). The electrolytes used for LNCO/LO, AC, KS6 electrodes, LICs and Li-DIBs were 1 M $LiPF_6$ dissolved in the mixed solvents of ethylene carbonate (EC), ethylmethyl carbonate (EMC) and dimethyl carbonate (DMC) (1:1:1 in volume) with 1% vinylene carbonate (VC) additives (LBC-305-01, CAPCHEM, marked A electrolytes). All cell assemblies were performed in a high pure Arfilled dry glovebox (MIKROUNA, O_2 and H_2O<0.1 ppm) and all tests were carried out at room temperature (about 25 ^oC). (The more detailed information of the above-mentioned chemicals, agents and materials can be seen the **Table S1**; the calculations for the m_+/m_-, C_m, E_m and P_m can be seen in the Methods.) Specifically, the galvanostatic charge-discharge tests (GCD) (rate, cycle) of LICs and Li-DIBs with anode presodiated at different current densities were on the Neware CT-4008 battery testing system. And the cyclic voltammetry (CV) and electrochemical impedance 6 spectroscopy (EIS) tests were carried out by means of the CHI-660E and CHI-440C electrochemical working stations.

Calculations for C_m, E_m, P_m

The specific capacity (C_m, mAh g^{-1}), energy density (E_m, Wh kg^{-1}) for LICs, energy density (E_m, Wh kg^{-1}) for Li-DIBs, and power density (P_m, kW kg^{-1}) were calculated according to the Equations **S**(1)-**S**(5).

$$m_+/m_- = 1:1 \quad (1)$$

$$C_m = Q / m \quad (2)$$

$$E_m \text{ (Capacitor)} = 0.5 (C_m \triangle V) \quad (3)$$

$$E_m \text{ (Battery)} = (C_m V) \quad (4)$$

$$P_m = 3.6 E_m / t_d \quad (5)$$

Where m, Q, $\triangle V$, V and t_d refer to the mass of active materials (mg) (for half cells, it means the mass of active materials of anode or cathode; for LICs and Li-DIBs full cells, it means the total masses of active materials of anode and cathode), specific charge or discharge capacity (mAh g^{-1}, for anode, it means the charge capacity; for cathode and full-cells, it refers to the discharge capacity), potential of the discharging plateaus (V), and discharging time (s), respectively.

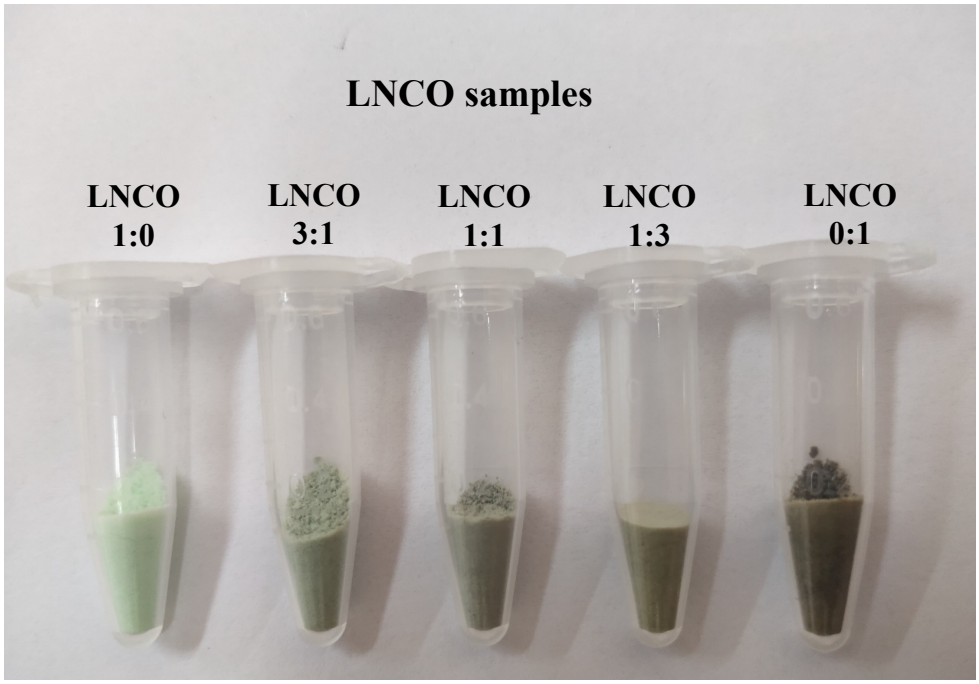

Fig S1. A picture of LNCO/LO(Ni:Co=1:0~0:1) precursor samples.

a

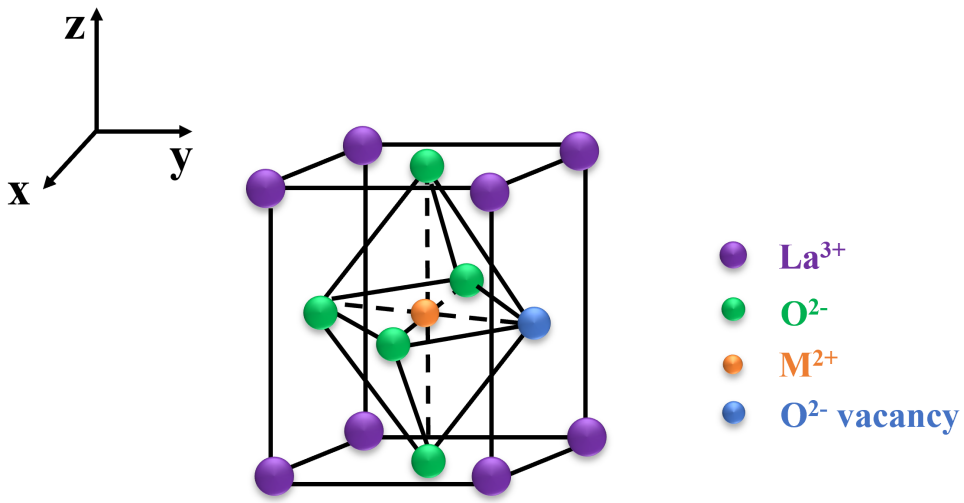

b

Sample	ICCD-PDF	Crystal system	Space group	Cell (a x b x c) / Å^3
$LaNiO_3$	34-1181	Hexagonal	R-Center	5.451×5.451×6.564
$LaCoO_3$	48-0123	Hexagonal	R-3c (167)	5.4445×5.4445×13.0936
La_2O_3	05-0602	Hexagonal	P-3m1(164)	3.9373×3.9373×6.1299

Fig S2. The crystal structures of perovskite $LaMO_3$ and detailed crystalline parameters for $LaNiO_3$ and $LaCoO_3$.

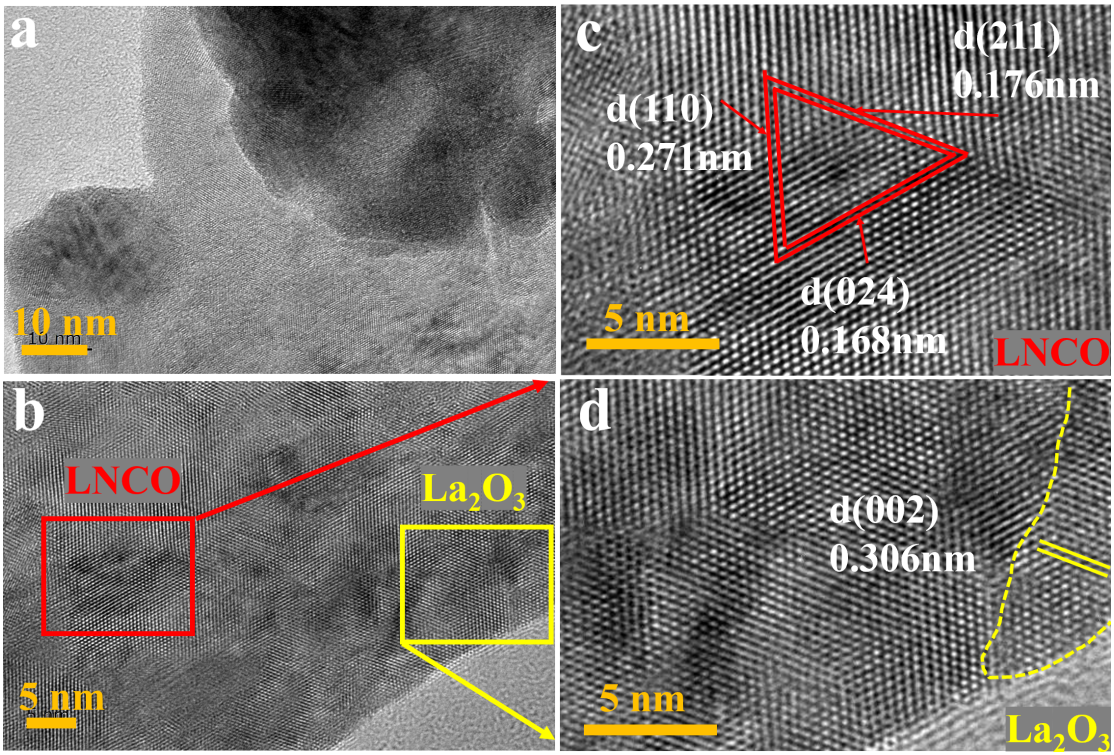

Fig S3. TEM and HRTEM of LNCO(1:3)/LO.

a

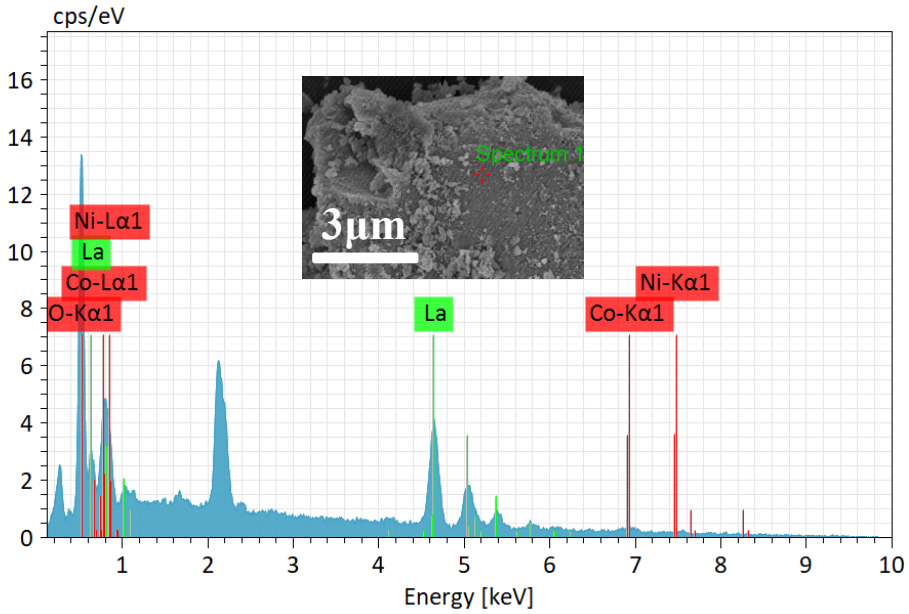

b

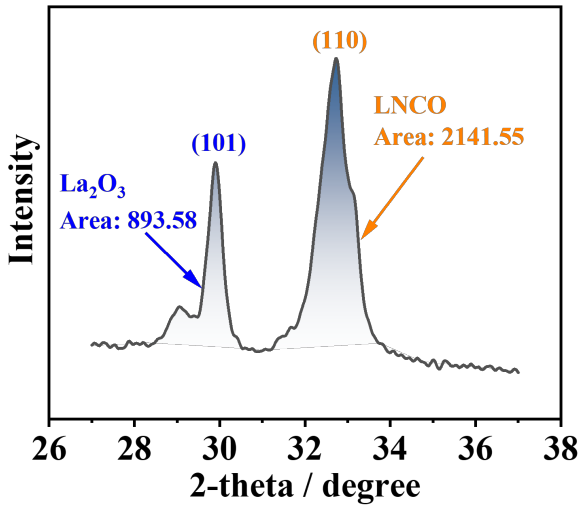

Fig S4. (a)EDS (Inset shows scanning spectrum) of LNCO(1:3). (b) XRD peak area fitting.

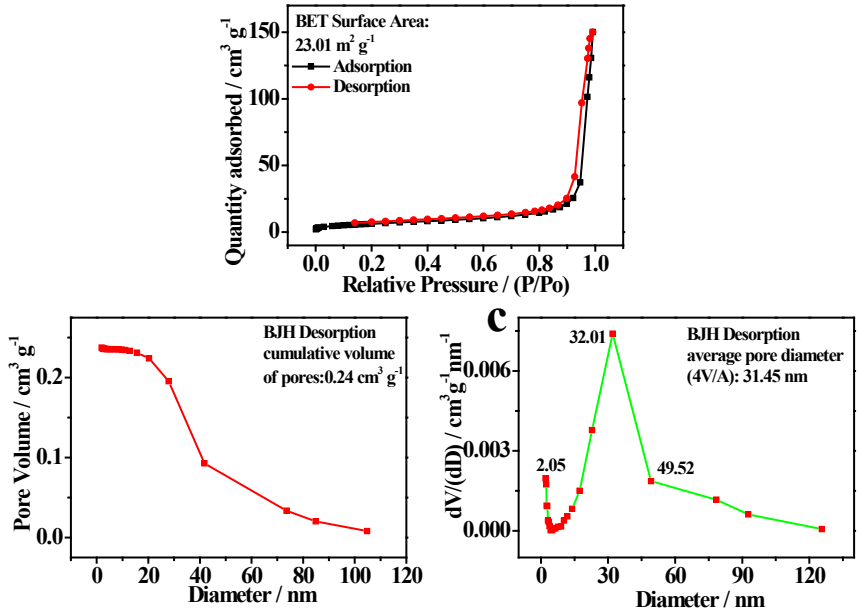

Fig S5. Nitrogen sorption isothermals (a), pore volume (b) and pore size distribution (c) of LNCO (1:3)/LO Sample.

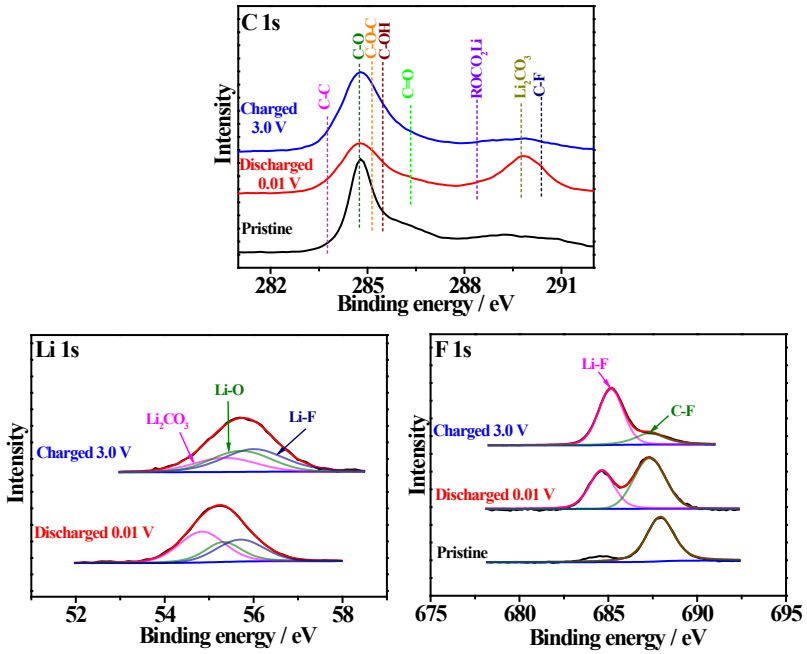

Fig S6. Ex-situ XPS spectra of LNCO(1:3)/LO pristine and discharged-0.01 V/charged-3.0 V states during the first discharging/charging cycle at 0.1 A g^{-1}: C1s-fitted (a), Li1s- fitted (b) and F1s-fitted (c).

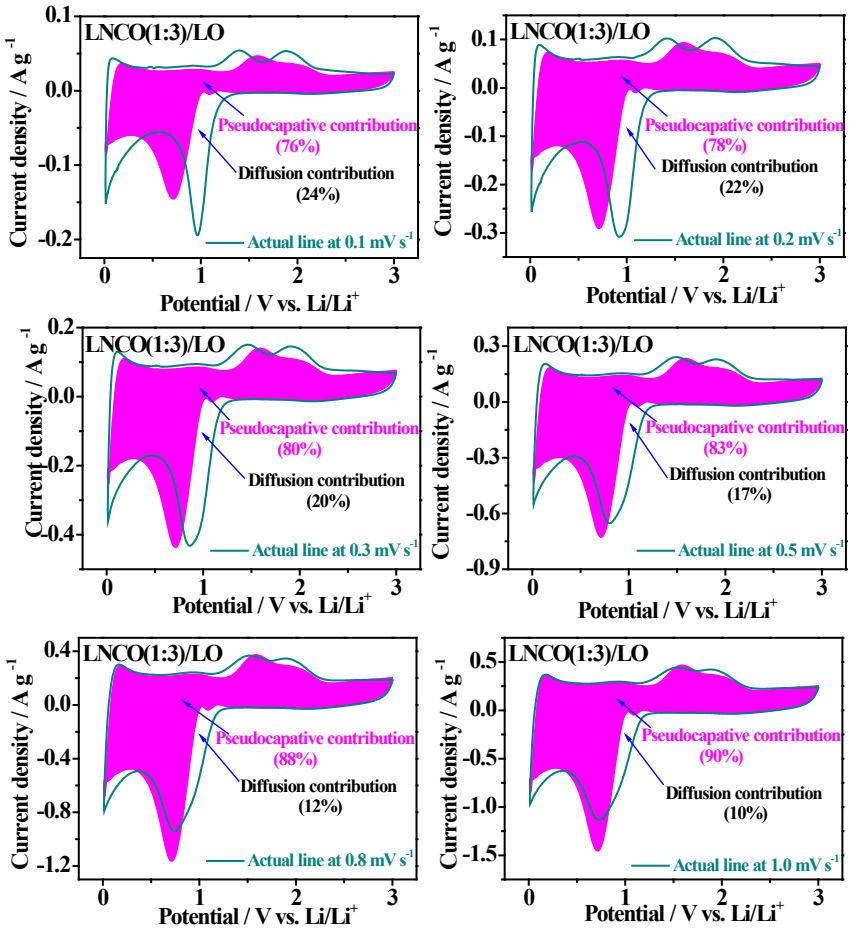

Fig S7. The pseudocapacitive and diffusion-controlled contributions to charge storage in the LNCO(1:3)/LO electrode (the shaded region is the identified pseudocapacitive contribution).

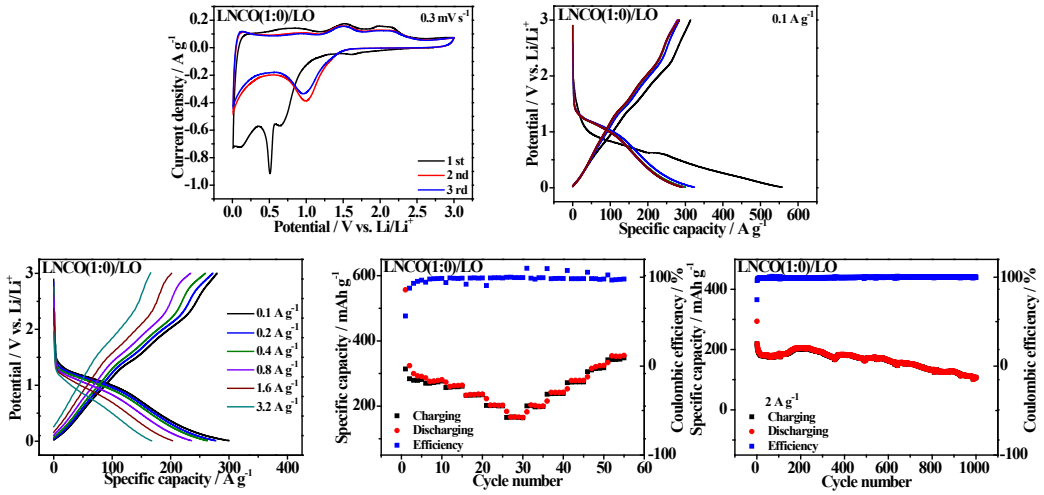

Fig S8. Performance of LNCO(1:0)/LO electrode with A electrolytes: CV plots for the first three cycles at 0.3 mV s^{-1} (a), GCD curves at 0.1 A g^{-1} for the first five cycles (b), GCD curves at 0.1-3.2 A g^{-1} (c), specific capacity and coulombic efficiency at 0.1-3.2 A g^{-1} (d), and cycling behavior at 2 A g^{-1} (e).

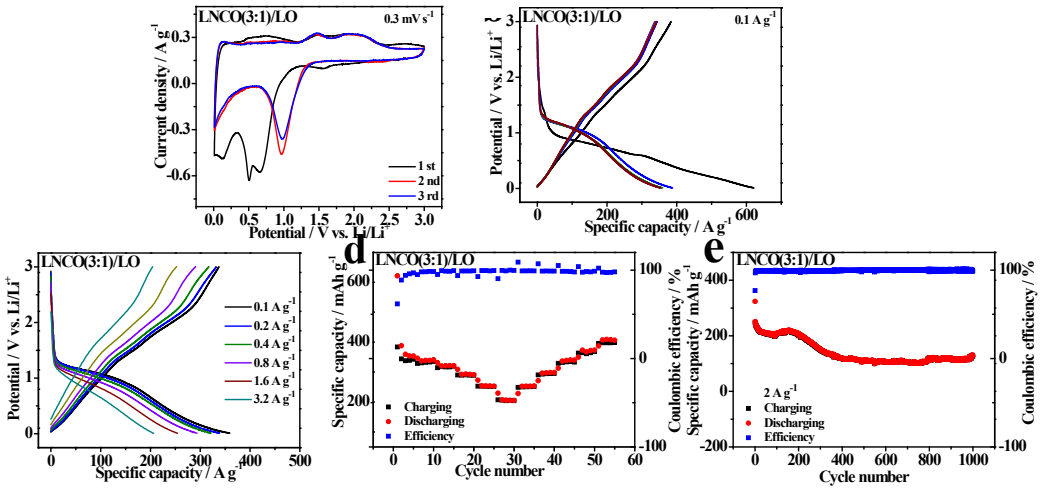

Fig S9. Performance of LNCO(3:1)/LO electrode with A electrolytes: CV plots for the first three cycles at 0.3 mV s^{-1} (a), GCD curves at 0.1 A g^{-1} for the first five cycles (b), GCD curves at 0.1-3.2 A g^{-1} (c), specific capacity and coulombic efficiency at 0.1-3.2 A g^{-1} (d), and cycling behavior at 2 A g^{-1} (e).

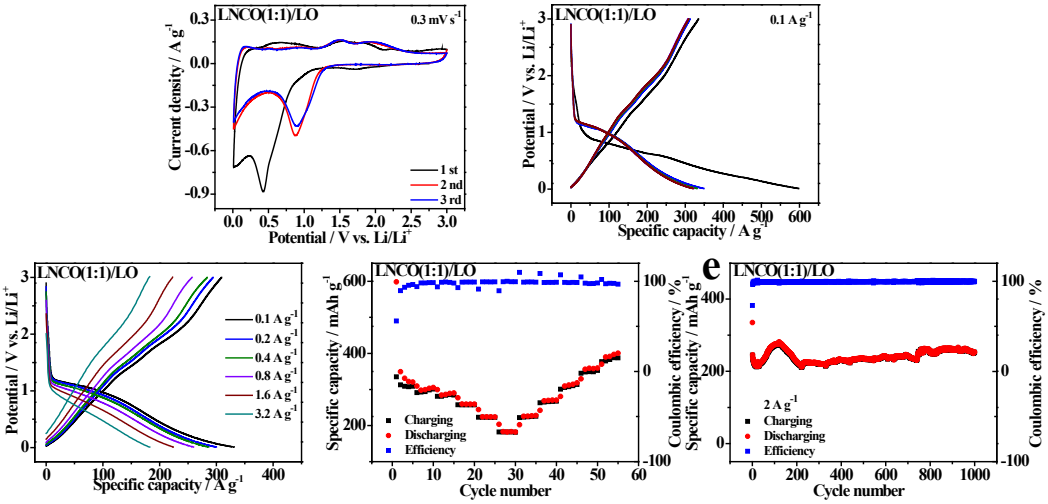

Fig S10. Performance of LNCO(1:1)/LO electrode with A electrolytes: CV plots for the first three cycles at 0.3 mV s^{-1} (a), GCD curves at 0.1 A g^{-1} for the first five cycles (b), GCD curves at 0.1-3.2 A g^{-1} (c), specific capacity and coulombic efficiency at 0.1-3.2 A g^{-1} (d), and cycling behavior at 2 A g^{-1} (e).

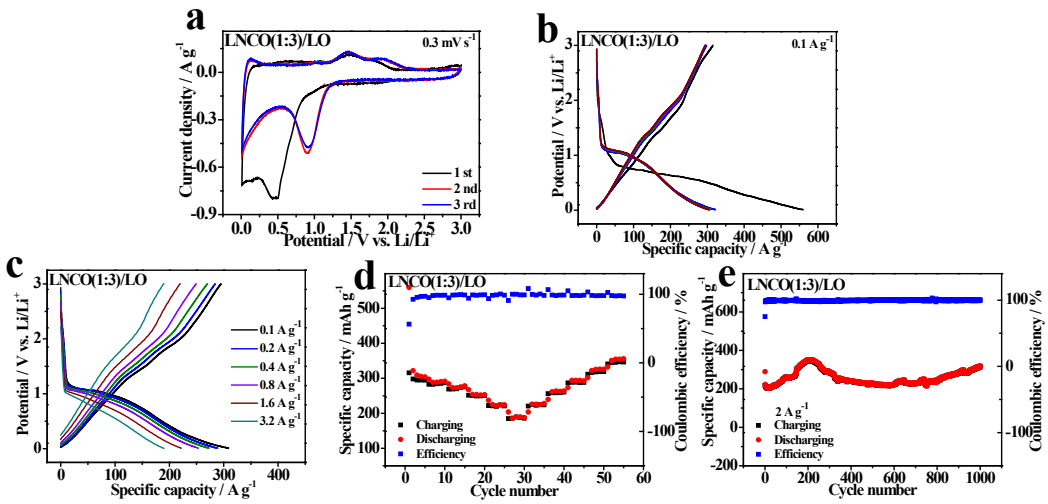

Fig S11. Performance of LNCO(1:3)/LO electrode with A electrolytes: CV plots for the first three cycles at 0.3 mV s^{-1} (a), GCD curves at 0.1 A g^{-1} for the first five cycles (b), GCD curves at 0.1-3.2 A g^{-1} (c), specific capacity and coulombic efficiency at 0.1-3.2 A g^{-1} (d), and cycling behavior at 2 A g^{-1} (e).

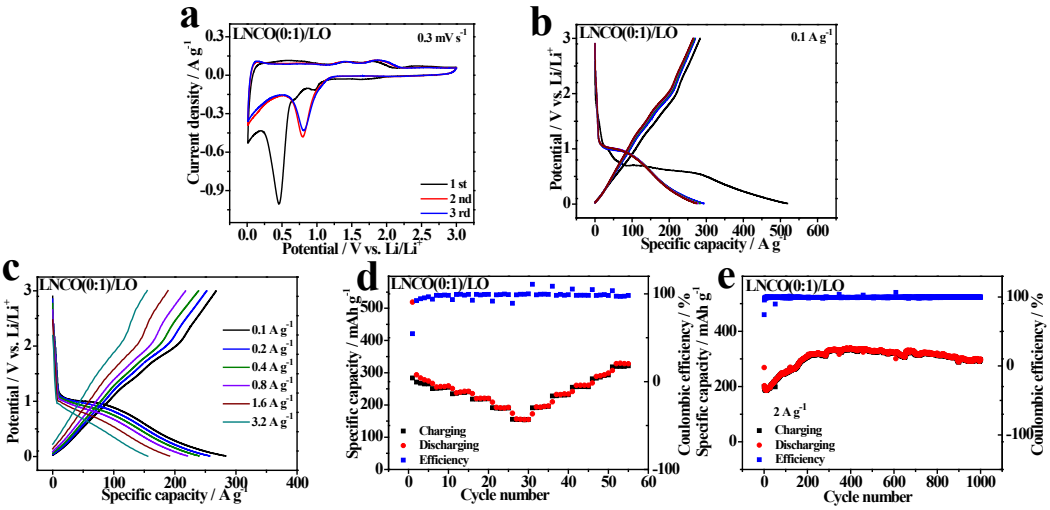

Fig S12. Performance of LNCO(0:1)/LO electrode with A electrolytes: CV plots for the first three cycles at 0.3 mV s^{-1} (a), GCD curves at 0.1 A g^{-1} for the first five cycles (b), GCD curves at 0.1-3.2 A g^{-1} (c), specific capacity and coulombic efficiency at 0.1-3.2 A g^{-1} (d), and cycling behavior at 2 A g^{-1} (e).

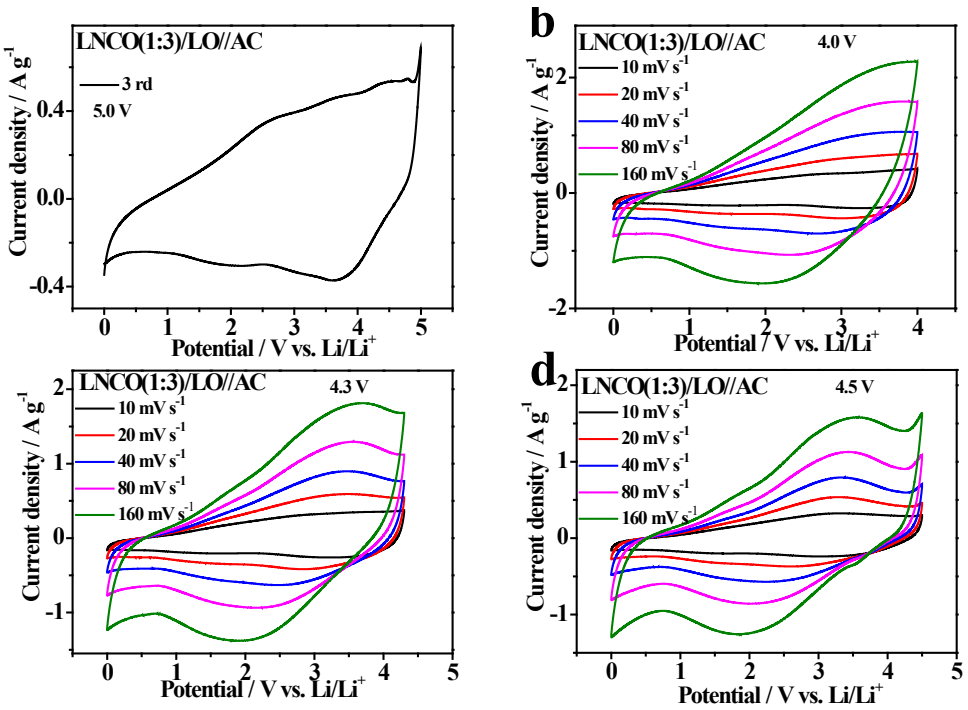

Fig S13. Performance of LNCO(1:3)/LO//AC LICs with A electrolytes: CV windows at 10 mV s^{-1} (a), CV plots at 10~160 mV s^{-1} in 4.0 V (b), 4.3 V (c), 4.5 V (d).

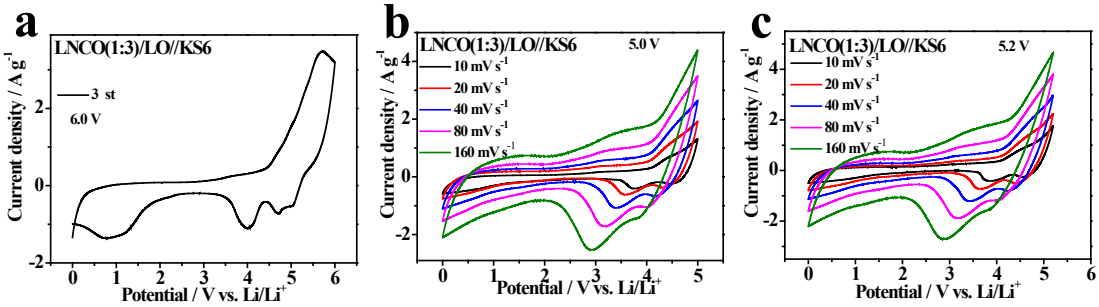

Fig S14. Performance of LNCO(1:3)/LO//KS6 DIBs with A electrolytes: CV windows at 10 mV s^{-1} (a), CV plots at 10~160 mV s^{-1} in 5.0 V (b), 5.2 V (c).

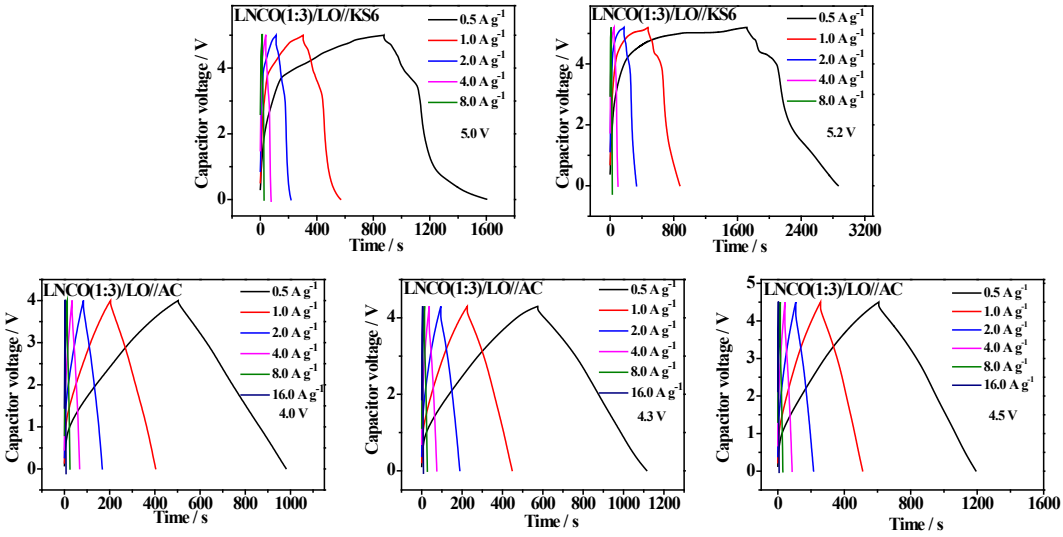

Fig S15. GCD curves of LNCO(1:3)/LO//KS6 DIBs and LNCO(1:3)/LO//AC LICs with A electrolytes: GCD curves at 0.5-8.0 A g^{-1} in 5.0 V (a), 5.2 V (b) of LNCO(1:3)/LO//KS6 Li-DIBs; GCD curves at 0.5-16.0 A g^{-1} in 4.0 V (c), 4.3 V (d), 4.5V (e) of LNCO(1:3)/LO//AC LICs.

Table S1. Chemicals, agents and materials used in the study.

Chemials, Agents and Materials	Type	Company	Characteristics
$La(NO_3)_3•xH_2O$	AR	SinoPharm	La_2O_3≥44%
$Ni(NO_3)_2•6H_2O$	AR	SinoPharm	purity≥98.0%
$Co(NO_3)_2•6H_2O$	AR	SinoPharm	purity≥98.5%
NaOH	AR	SinoPharm	purity≥96.0%
Na_2CO_3	AR	SinoPharm	purity≥99.8%
AC	YEC 8b	FuZhou YiHuan	D50: ~10 μm; Density: 0.4 g cm^{-3}; SSA:2000~2500 m^2 g^{-1}
Graphite	KS6	TiMCAL	D90: 5.8-7.1 μm; Interlayer distance: 0.3354-0.3360 nm; SSA: 20 m^2 g^{-1}; Density-Scott: 0.07 g cm^{-3};
AB	Battery grade		/
NMP	AR	Kermel	purity≥99.0%
PVDF	Battery grade		/
Electrolytes	LBC-305-01	CAPCHEM	1 M $LiPF_6$/EC:EMC:DMC (1:1:1) /1% VC
Li plate	15.6*0.45 mm	China Energy	15.6*0.45 mm
Cu foil	200*0.015	GuangZhou JiaYuan	Total thickness: 15 μm; weight: 87 g m^{-2}
Carbon coated-Al foil	222*0.015	GuagZhou NaNuo	Total thickness: 17 μm; Strength: 192 Mpa
Glass microfiber filters	GF/D 2.7 μm; 1823-025	Whatman	Diameter: 25 mm; Thickness: 675 μm; weight: 121 g m^{-2}
Cell components	CR-2032	ShenZhen TianChenHe	/

Table S2. Specific capacity and cycling retention of the LNCO/LO(Ni:Co=1:0~0:1) electrodes.

	Specific capacity of LNCO/LO(1:0~0:1) electrodes / (mAh g^{-1})				
Current density / (A g^{-1})	**1:0**	**3:1**	**1:1**	**1:3**	**0:1**
0.1	279.2	337.5	309.1	294.9	267.6
0.2	272.0	332.3	294.2	284.3	252.2
0.4	259.4	317.1	284.0	270.0	238.9
0.8	233.9	290.2	257.1	249.3	217.8
1.6	201.4	252.3	223.0	219.5	189.3
3.2	166.2	204.4	182.1	189.3	154.7
Cycling behavior Retention% / 2 A g^{-1} / 1000 cycles	48%	51%	103%	146%	148%

Table S3. Specific capacity cycling retention of AC and KS6 electrodes.

	Specific capacity of Positive electrodes / (mAh g^{-1})	
Current density / (A g^{-1})	**AC**	**KS6**
0.1	86.3	91.5
0.2	74.1	74.3
0.4	66.0	71.0
0.8	58.9	66.4
1.6	52.4	58.2
3.2	46.2	41.8
Cycling behavior Retention% / 1 A g^{-1} / 1000 cycles	77%	84%

Table S4. Performance summary of the LICs and Li-DIBs in the study under room temperature (25 ^{o}C), m^{+}/m^{-}=1:1.

Type	Capacitor or Cell system	Working voltage / V	Energy density / Wh kg^{-1}	Power density / kW kg^{-1}	Cycling behavior / retention%, repeated cycles, current density
LICs	LNCO(1:3) /LO//AC	0.01-4.0	66.1-55.4 46.3-37.5 26.7-15.6	0.5-1.0 2.0-4.0 8.0-16.0	85%/1000/5 A g^{-1} 83%/2000/5 A g^{-1} 74%/3000/5 A g^{-1} 77%/4000/5 A g^{-1} 68%/5000/5 A g^{-1}
		0.01-4.3	80.6-66.5 56.2-44.6 33.2-21.0	0.5-1.0 2.2-4.3 8.6-17.2	56%/1000/5 A g^{-1} 52%/2000/5 A g^{-1} 40%/3000/5 A g^{-1} 33%/4000/5 A g^{-1} 30%/5000/5 A g^{-1}
		0.01-4.5	87.1-75.6 63.9-51.5 36.3-19.1	0.5-1.0 2.2-4.3 8.6-17.2	52%/1000/5 A g^{-1} 43%/2000/5 A g^{-1} 40%/3000/5 A g^{-1} 38%/4000/5 A g^{-1} 37%/5000/5 A g^{-1}
Li-DIBs	LNCO(1:3) /LO//KS6	0.01-5.0	116.2-99.4 72.9-52.8-36.1	0.6-1.4 2.5-5.0-10.0	93%/100/2 A g^{-1} 88%/200/2 A g^{-1} 81%/300/2 A g^{-1} 70%/400/2 A g^{-1} 60%/500/2 A g^{-1} 37%/1000/2 A g^{-1}
		0.01-5.2	206.0-166.3 114.0-69.3-40.4	0.6-1.5 2.6-5.2-10.4	60%/100/2 A g^{-1} 49%/200/2 A g^{-1} 39%/300/2 A g^{-1} 29%/400/2 A g^{-1} 22%/500/2 A g^{-1} 12%/1000/2 A g^{-1}

Table S5. A comparison for the performance of the LNCO(1:3)/LO//AC LICs in the study with some reported LICs.

LICs	Working voltage/ V	Energy density / Wh kg^{-1}	Power density / kW kg^{-1}	Cycling behavior / retention%, repeated cycles, current density	Refs.
Li_3VO_4/N-C//AC	1.0-4.0	136.4-24.4	0.53-11	87%/1500/2 A g^{-1}	1
$TiNb_2O_7$@C//CFs	0.8-3.2	110.4-20	0.1-5.46	77%/1500/0.2 A g^{-1}	2
MnO@C//PC	0.1-4.0	117.6-27.8	0.4-10.2	76%/5000/1 A g^{-1}	3
AC/TiO_2@PCNF-12	0.0-3.0	67.4-27.5	0.075-5	85%/10000/10 A g^{-1}	4
AC-HBP//LiC_6	2.0-3.9	100-20	0.3-2	70%/2000/0.5 A g^{-1}	5
TiO_2/graphene//AC	1.0-3.0	42-8.9	0.8-8	100%/6500/4 A g^{-1}	6
H-TiO2/PPy/SWCNTs//AC	1.0-3.0	31.3-1.9	0.2-4.0	77.8%/3000/0.5 A g^{-1}	7
SnO_2-C//C	0.5-4.0	110-45	0.19-2.96	80%/2000/1 A g^{-1}	8
Graphene-VN//cabron nanorods	0.0-4.0	162-64	0.2-10	83%/1000/2 A g^{-1}	9
T-Nb_2O_5/Graphene paper//AC	0.5-3.0	47-15	0.39-18	93%/2000/0.25 A g^{-1}	10
Fe_3O_4/Graphene// Graphene	1.0-4.0	147-86	0.15-2.5	70%/1000/2 A g^{-1}	11
LNCO(1:3)/LO//AC	**0.01-4.0**	**66.1-55.4 46.3-37.5 26.7-15.6**	**0.5-1.0 2.0-4.0 8.0-16.0**	**85%/1000/5 A g^{-1} 83%/2000/5 A g^{-1} 74%/3000/5 A g^{-1} 77%/4000/5 A g^{-1} 68%/5000/5 A g^{-1}**	**This work**

Table S6. A comparison for the performance of the LNCO(1:3)/LO//KS6 Li-DIBs in the study with some reported Li-DIBs.

Li-DIBs	Working voltage/ V	Energy density / Wh kg^{-1}	Power density / kW kg^{-1}	Cycling behavior / retention%, repeated cycles, current density	Refs.
Graphite//Graphite	0.01-5.2	108		67%/50/0.05 A g^{-1}	12
Si-compound//Graphite	0-3	54		53%/100/0.1 A g^{-1}	13
Nb_2O_5//Graphite	1.5-3.5	52		84%/100/0.1 A g^{-1}	14
TiO_2//Graphite	1.5-3.7	36		88%/50/0.1 A g^{-1}	15
MoO_3//Graphite	1.5-3.5	77		90%/200/0.081 A g^{-1}	16
AC//Graphite	0-3.5	150		98% /100 /1.86 mA cm^{-2}	17
Graphite//Graphite	3-5	170		94%/500/0.5 A g^{-1}	18
Al//Graphite	3.0-5.0	150	1.2	98%/600/0.2 A g^{-1}	19
MTI//KS6-DIB	3.0-5.1	125	0.4	90%/200/0.5 A g^{-1}	20
LNCO(1:3)/LO//KS6	**0.01-5.0**	**116.2-99.4 72.9-52.8-36.1**	**0.6-1.4 2.5-5.0-10.0**	**93%/100/2 A g^{-1} 88%/200/2 A g^{-1} 81%/300/2 A g^{-1} 70%/400/2 A g^{-1} 60%/500/2 A g^{-1} 37%/1000/2 A g^{-1}**	**This work**

References

1. L. F. Shen, H. F. Lv, S. Q. Chen, P. Kopold, P. A. van Aken, X. J. Wu, J. Maier and Y. Yu, *Adv. Mater.*, 2017, **29**, 1700142.
2. X. F. Wang and G. Z. Shen, *Nano Energy*, 2015, **15**, 104-115.
3. D. Yan, S.-H. Li, L.-P. Guo, X.-L. Dong, Z.-Y. Chen and W.-C. Li, *ACS Appl. Mater. Interfaces*, 2018, **10**, 43946-43952.
4. C. Yang, J.-L. Lan, W.-X. Liu, Y. Liu, Y.-H. Yu and X.-P. Yang, *ACS Appl. Mater. Interfaces*, 2017, **9**, 18710-18719.
5. A. Jain, S. Jayaraman, M. Ulaganathan, R. Balasubramanian, V. Aravindan, M. P. Srinivasan and S. Madhavi, *Electrochim. Acta*, 2017, **228**, 131-138.
6. H. Kim, M. Y. Cho, M. H. Kim, K. Y. Park, H. Gwon, Y. Lee, K. C. Roh and K. Kang, *Adv. Energy Mater.*, 2013, **3**, 1500-1506.
7. G. Tang, L. J. Cao, P. Xiao, Y. H. Zhang and H. Liu, *J. Power Sources*, 2017, **355**, 1-7.
8. W.-H. Qu, F. Han, A.-H. Lu, C. Xing, M. Qiao and W.-C. Li, *J. Mater. Chem. A*, 2014, **2**, 6549-6557.
9. R. T. Wang, J. W. Lang, P. Zhang, Z. Y. Lin and X. B. Yan, *Adv. Funct. Mater.*, 2015, **25**, 2270-2278.
10. L. P. Kong, C. F. Zhang, J. T. Wang, W. M. Qiao, L. C. Ling and D. H. Long, *ACS Nano*, 2015, **9**, 11200-11208.
11. F. Zhang, T. F. Zhang, X. Yang, L. Zhang, K. Leng, Y. Huang and Y. S. Chen, *Energy Environ. Sci.*, 2013, **6**, 1623-1632.
12. J. A. Read, A. V. Cresce, M. H. Ervin and K. Xu, *Energy Environ. Sci.*, 2014, **7**, 617-620.
13. H. Nakano, Y. Sugiyama, T. Morishita, M. J. S. Spencer, I. K. Snook, Y. Kumai and H. Okamoto, *J. Mater. Chem. A*, 2014, **2**, 7588-7592.
14. G. Park, N. Gunawardhana, C. Lee, S.-M. Lee, Y.-S. Lee and M. Yoshio, *J. Power Sources*, 2013, **236**, 145-150.
15. A. K. Thapa, G. Park, H. Nakamura, T. Ishihara, N. Moriyama, T. Kawamura, H. Wang and M. Yoshio, *Electrochim. Acta*, 2010, **55**, 7305-7309.
16. N. Gunawardhana, G.-J. Park, N. Dimov, A. K. Thapa, H. Nakamura, H. Wang, T. Ishihara and M. Yoshio, *J. Power Sources*, 2011, **196**, 7886-7890.
17. T. Ishihara, Y. Yokoyama, F. Kozono and H. Hayashi, *J. Power Sources*, 2011, **196**, 6956-6959.
18. S. Rothermel, P. Meister, G. Schmuelling, O. Fromm, H.-W. Meyer, S. Nowak, M. Winter and T. Placke, *Energy Environ. Sci.*, 2014, **7**, 3412-3423.

19. X. L. Zhang, Y. B. Tang, F. Zhang and C. S. Lee, *Adv. Energy Mater.*, 2016, **6**, 1502588.

20. C. Y. Chan, P.-K. Lee, Z. Xu and D. Y. W. Yu, *Electrochim. Acta*, 2018, **263**, 34-39.